

Northumbria Research Link

Citation: Wu, Dong, Zhao, Jue, Su, Yinglong, Yang, Mengjie, Dolfing, Jan, Graham, David W., Yang, Kai and Xie, Bing (2023) Explaining the resistomes in a megacity's water supply catchment: Roles of microbial assembly-dominant taxa, niched environments and pathogenic bacteria. *Water Research*, 228 (Part A). p. 119359. ISSN 0043-1354

Published by: Elsevier

URL: <https://doi.org/10.1016/j.watres.2022.119359>
<<https://doi.org/10.1016/j.watres.2022.119359>>

This version was downloaded from Northumbria Research Link:
<https://nrl.northumbria.ac.uk/id/eprint/51004/>

Northumbria University has developed Northumbria Research Link (NRL) to enable users to access the University's research output. Copyright © and moral rights for items on NRL are retained by the individual author(s) and/or other copyright owners. Single copies of full items can be reproduced, displayed or performed, and given to third parties in any format or medium for personal research or study, educational, or not-for-profit purposes without prior permission or charge, provided the authors, title and full bibliographic details are given, as well as a hyperlink and/or URL to the original metadata page. The content must not be changed in any way. Full items must not be sold commercially in any format or medium without formal permission of the copyright holder. The full policy is available online: <http://nrl.northumbria.ac.uk/policies.html>

This document may differ from the final, published version of the research and has been made available online in accordance with publisher policies. To read and/or cite from the published version of the research, please visit the publisher's website (a subscription may be required.)

1 **Explaining the resistomes in a megacity's water supply catchment: Roles of microbial**
2 **assembly-dominant taxa, niched environments and pathogenic bacteria**

3

4 Dong Wu^{1,2,3}, Jue Zhao⁴, Yinglong Su^{1,3}, Mengjie Yang¹, Jan Dolfing⁵, David W. Graham^{6*},
5 Kai Yang^{1,3*}, Bing Xie^{1,3*}

6

7 ¹ Shanghai Engineering Research Center of Biotransformation of Organic Solid Waste,
8 Shanghai Key Lab for Urban Ecological Processes and Eco-Restoration, School of Ecological
9 and Environmental Sciences, East China Normal University, Shanghai 200241, PR China

10 ² Key Laboratory of Environmental Pollution Monitoring and Disease Control, Ministry of
11 Education, Guizhou Medical University, Guizhou 550001, PR China

12 ³ Shanghai Institute of Pollution Control and Ecological Security, Shanghai 200092, PR China

13 ⁴ Department of Civil and Environmental Engineering and Research Institute for Sustainable
14 Urban Development, The Hong Kong Polytechnic University, Kowloon, Hong Kong

15 ⁵ Faculty Energy and Environment, Northumbria University, Newcastle upon Tyne, NE1 8QH,
16 UK

17 ⁶ School of Engineering, Newcastle University, Newcastle upon Tyne, NE1 7RU, UK

18

19 *Corresponding authors:

20 Prof. Bing Xie; East China Normal University; Shanghai 200241, P.R. China. Email:
21 bxie@des.ecnu.edu.cn; Phone: (+86) 021-54341276.

22

23 Prof. Kai Yang; East China Normal University; Shanghai 200241, P.R. China. Email:
24 kyang@re.ecnu.edu.cn; Phone: (+86) 021-54341069

25

26 Prof. David W Graham, Newcastle University; Newcastle upon Tyne, United Kingdom. Email:
27 david.graham@ncl.ac.uk; Phone: (+44) 0191-208-7925

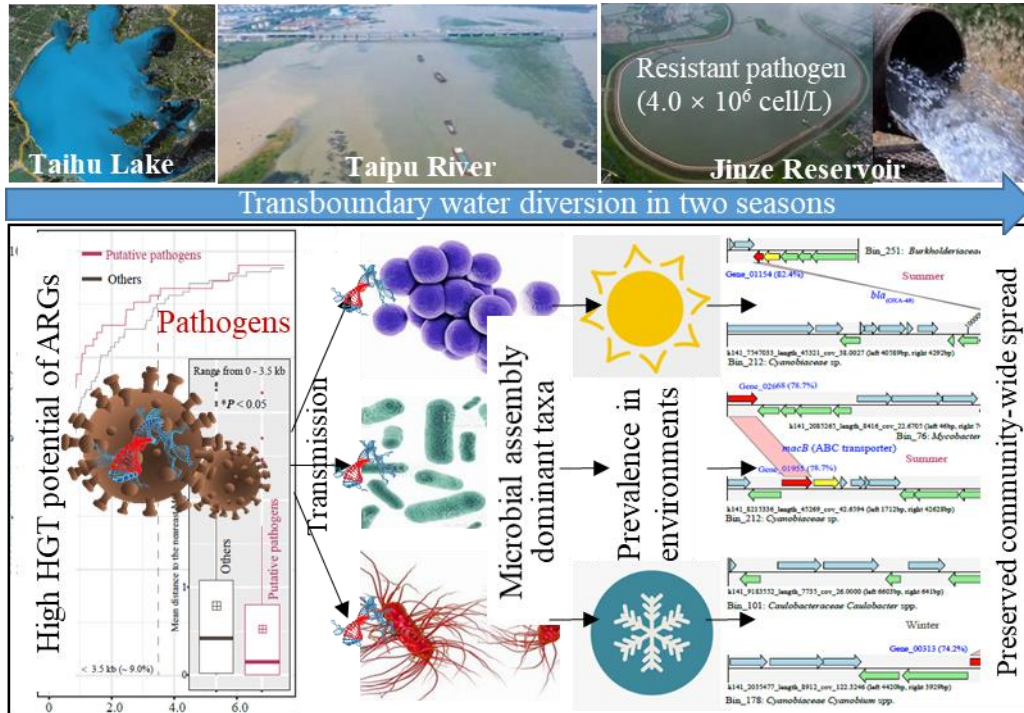
28

29

Highlights

- Resistome size in the reservoir was comparable to that in sewers
- Microbial assembly process significantly influenced dynamics of resistome
- Putative resistant bacteria were at the same abundance across the catchment
- Putative resistant pathogens greatly contributed to the transmission of ARGs
- Intragenomic ARGs frequently transferred to microbial assembly-dominant taxa

Graphic Abstract



30 Abstract

31 Antibiotic resistance genes (ARGs) in drinking water sources suggest the possible presence of
32 resistant microorganisms that jeopardize human health. However, explanations for the presence
33 of specific ARGs in situ are largely unknown, especially how their prevalence is affected by
34 local microbial ecology, taxa assembly and community-wide gene transfer. Here, we
35 characterized resistomes and bacterial communities in the Taipu River catchment, which feeds
36 a key drinking water reservoir to a global megacity, Shanghai. Overall, ARG abundances
37 decreased significantly as the river flowed downstream towards the reservoir ($P < 0.01$),
38 whereas the waterborne bacteria assembled deterministically ($|\beta\text{NRI}| > 2.0$) as a function of
39 temperature and dissolved oxygen conditions with the assembly-dominant taxa (*e.g.*
40 *Ilumatobacteraceae* and *Cyanobiaceae*) defining local resistomes ($P < 0.01$, Cohen's D = 4.22).
41 Bacterial hosts of intragenomic ARGs stayed at the same level across the catchment (60 ~ 70
42 genome copies per million reads). Among them, the putative resistant pathogens (*e.g.*
43 *Burkholderiaceae*) carried mixtures of ARGs that exhibited high transmission probability
44 (transfer counts = 126, $P < 0.001$), especially with the microbial assembly-dominant taxa.
45 These putative resistant pathogens had densities ranging from 3.0 to 4.0×10^6 cell/L, which
46 was more pronouncedly affected by resistome and microbial assembly structures than
47 environmental factors (SEM, std-coeff $\beta = 0.62$ vs. 0.12). This work shows that microbial
48 assembly and resistant pathogens play predominant roles in prevalence and dissemination of
49 resistomes in receiving water, which deserves greater attention in devising control strategies for
50 reducing in-situ ARGs and resistant strains in a catchment.

51 **Keywords:** antibiotic resistance, community-wide gene transfer, putative resistant pathogen,
52 metagenome binning, microbial assembly, water supply catchment

53

54 **Abbreviations**

- 55 • Antibiotic resistance (AR)
- 56 • Aminoglycosides (Agy)
- 57 • Antibiotic resistance genes (ARGs)
- 58 • Average nucleotide identity (ANI)
- 59 • Bacitracin (Bac)
- 60 • Beta(β)-lactams (Bla)
- 61 • Chloramphenicol (Cp)
- 62 • Horizontal gene transfer (HGT)
- 63 • Fecal coliform (FC)
- 64 • Fluoroquinolones (Fq)
- 65 • Macrolides (Mls)
- 66 • Metagenome-assembled genomes (MAGs)
- 67 • Mobile genetic elements (MGEs)
- 68 • Open reading frames (ORFs)
- 69 • Peptides (Ptd)
- 70 • Polymerase chain reaction (PCR)
- 71 • Polymyxins (Pmx)
- 72 • Multidrug resistance (MDR)
- 73 • Rifamycin (Rmc)
- 74 • Sulfonamides (Sa)
- 75 • Tetracyclines (Tc)
- 76

77 **1. Introduction**

78 Antibiotic resistance (AR) is natural and ancient (D'Costa *et al.* 2011). As opposed to dogma
79 that views the presence of antibiotic resistance genes (ARGs) in a place as the consequence of
80 selective pressures, growing literature suggests that the microbial ecological context and niches
81 may be more important to local ARG prevalence in natural and anthropogenic settings
82 (Mahnert *et al.* 2019, Pehrsson *et al.* 2016). However, the niche-influenced assembly depend
83 on various factors, such as microbial phylogenetic and taxonomic structures in human gut
84 (Smillie *et al.* 2011), salinity in soil (Tan *et al.* 2019), microplastics in rivers (Wang *et al.* 2020),
85 and particles in the air (Xie *et al.* 2019). Strong evidence further suggests that the spread of
86 ARGs is affected by microbial and environmental variables related to mobile genetic elements
87 (MGEs) (Quintela-Baluja *et al.* 2021, Su *et al.* 2015, Wu *et al.* 2019).

88 As such, different studies have broadly applied this 'microbe-environment-MGE' triad co-
89 driven theory to explain the dynamics of resistomes in riverine, atmospheric, soil and
90 wastewater environments (Gibson *et al.* 2015, Quintela-Baluja *et al.* 2019, Zhu *et al.* 2021,
91 Zhu *et al.* 2017), and even in pristine Arctic areas (McCann *et al.* 2019). However, the specific
92 roles of microbial assembly featured key taxa (Munck *et al.* 2015), pertinent environmental
93 conditions (Sun *et al.* 2020), and MGE-mediated gene transfer (Quintela-Baluja *et al.* 2021)
94 playing in local resistomes have yet to be holistically analyzed (Larsson *et al.* 2018, Winter *et*
95 *al.* 2021).

96 A flowing water supply catchment contains a series of distinctive microbial structures (Chen
97 *et al.* 2020) and spatial ecosystems (Maavara *et al.* 2017), and is a useful platform for tracking
98 ARG distribution and analyzing 'microbe-environment-MGE' co-driven mechanisms (Amos
99 *et al.* 2018). A recent study showed that representative taxa groups in different compartments
100 of a wastewater network imposed different selection effects on resistomes across a 'sewer to

101 river' continuum (Quintela-Baluja *et al.* 2019). But notably, to detect and analyze the dynamics
102 of these niche compartment-specific bacterial taxonomic assemblages, few studies have
103 included ecological assembly-based models (Ning *et al.* 2020), nor considered the in-situ
104 microbial ecology driven environment-filtering effects (Yan *et al.* 2016).

105 MGEs can be useful biomarkers for AR in water catchments (Quintela-Baluja *et al.* 2021).
106 MGE-laden ARGs, frequently associated with human allochthonous pathogens (Forsberg *et al.*
107 2012), often relate greater horizontal gene transfer (HGT) potential (D'Costa *et al.* 2006).
108 Therefore, a generally greater prevalence of waterborne ARGs and MGEs exist in places with
109 greater anthropogenic impact (Elder *et al.* 2021, Liang *et al.* 2019). However, clinically
110 important ARGs (*e.g.* *bla*_{CTX-M} and *mcr-1*) hosted by potential pathogens, like *Enterobacteria*,
111 *Aeromonads*, and *V. cholera*, have also been observed in places where human impacts are less
112 apparent (Chen *et al.* 2019, Dang *et al.* 2020, Rysz *et al.* 2013, Walsh *et al.* 2011). This prompts
113 the speculation of a continuous ARG-transfer between the microbial assembly-dominant taxa,
114 which constantly exist in the ecosystem at high abundances, and human-associated
115 microbiomes (Forsberg *et al.* 2014, Hassan *et al.* 2021, Ning *et al.* 2020). However, between
116 human pathogens and assembly-dominant taxa, the intragenomic transfer of 'ARG - MGE'
117 matching pairs have not been evidenced at the community-wide scale yet, especially in the
118 water supply catchment.

119 Here, we study the main drinking water supply catchment of Shanghai, the largest city in China,
120 to better understand how microbial dynamics and environmental drivers impact in-situ
121 resistomes across a catchment. Using high throughput metagenomic sequencing, microbial
122 community assembly modeling, genome binning related bioinformatics and cell quantification
123 techniques, three goals were achieved: i) detecting and analyzing the hypothesized dominance
124 of microbial assembly over the dynamics of resistome; ii) elucidating the hypothetical ARG

125 transfer between the microbial assembly-dominant taxa and putative human allochthonous
126 pathogens via genome-warranted approaches; and iii) quantifying density of putative
127 pathogenic ARG-hosts and estimating potential hazards exposed to the catchment users across
128 seasons and geographic gradients.

129 **2. Materials and methods**

130 *2.1 Study areas, sampling, and measurement of physicochemical parameters*

131 There were six sampling sites in the studied watershed (**Fig. 1a**), including Taihu Lake pumping
132 station (TP) as the origin; Pingwang Station (PW), Lili Station (LL), and Luxu Station (LX) in
133 Taihu River; and the inlet (JRi) and outlet of Jinze Reservoir (JRe), which provides drinking
134 water to 24 million Shanghai citizens. The sampling campaign was commenced in parallel with
135 Taihu Basin Management Authority's transboundary water diversion from Taihu Lake in
136 Jiangsu Province to the downstream Taihu River towards Shanghai, from June to September
137 2019 (summer) and November 2019 to February 2020 (winter). A total of 180 individual
138 samples (5 replica×36) were collected along the water catchment. At each sampling site, five
139 replicas (200mL) within a 3 - 5 km sampling region (0.5 to 1.0m in depth) were collected by
140 using a Schindler sampler and then were combined to a sterile PE bottle (1L) before being
141 transferred in the lab for vacuum filtration. Specific information, including sample pretreatment,
142 sampling date, and exact locations are provided in Supplementary Information (**SI-1**).

143 The pretreated water samples (after settling) were used for the measurement of COD, BOD₅,
144 total nitrogen, total phosphorus, and nitrate using an automated discrete analyzer (SmartChem-
145 200, Italy). Handheld instruments were used to detect temperature, pH (PH-Scan, Shanghai),
146 and dissolved oxygen (DO) (HI9147, Hanna, Italy) on site. Fecal coliform (FC) levels were
147 measured for pretreated water samples on the sampling day, according to previously published

148 culturing methods (Lamba *et al.* 2017).

149 2.2 DNA extraction, 16S rRNA gene and metagenomic sequencing

150 DNA was extracted from vacuum-filtered biosolids collected using sterile 0.22-mm membrane
151 disc filters (Supor® Membrane, Pall Co., USA). Extraction was performed using Power Soil
152 DNA extraction kits (MOBio, USA) and a Ribolyzer (FastPre-24, MP, US), according to
153 manufacturers' suggested protocols. The quality checked samples were sent to Personal
154 Biotech Company Ltd. (Shanghai, China) for library construction (size = 250 bp) and then were
155 applied for 16S rRNA gene (V4 region) amplicon and metagenomic sequencing on the platform
156 of Illumina-NovaSeq (Illumina, USA). The raw sequences were submitted to The National
157 Center for Biotechnology Information (NCBI). The sequence read archive (SRA) can be
158 retrieved via the accession numbers PRJNA730720 (metagenomics sequences) and
159 PRJNA767498 (16S rRNA sequences). Details of primers, library construction and
160 metagenomic sequencing were provided in Supplementary Information (SI-2)

161 2.3 Profile of resistome, dynamics of bacterial community and predicted function

162 Raw data were initially processed using FASTP to remove low-quality ($\geq Q20$, length > 150 bp)
163 sequencing reads, which were analyzed by ARG-oap (v2.3) pipelines to map the mosaic of
164 resistome (id = 80%, threshold value = 10^{-10}). The relative abundances of detected ARGs
165 were normalized to the copy numbers of (per) identified 16S rRNA genes showing the
166 prevalence of genes (Yang *et al.* 2016). All samples' 16S rRNA amplicon sequences were
167 analyzed by Qiime2-DADA2 (v2020.11) to generate sequence variant (ASV) tables, the
168 taxonomy of which were assigned by using the closed reference approach, against the trained
169 SILVA 138 database. The rarefied BIOM table was further processed to remove the ASVs
170 occurring in less than 10% of the samples ($n = 4$) with frequencies no less than one. To analyze

171 the microbial community assembly structures relative to environmental filtering effects,
172 phylogenetic bin-based null model analysis (iCAMP) was utilized (Ning *et al.* 2020); the bin
173 size and ses.cut (β NRI/NTI) thresholds of each season group were set as 24 and 1.96,
174 respectively. The taxonomic groups mostly contributing to the iCAMP-identified process were
175 regarded as the assembly-dominant taxa (significant phylogenetic signal < 0.05). The
176 metabolic functions of the microbial community were predicted by using FAPROTAX
177 pipelines that were constructed with a database specific to prokaryotic taxa (Louca *et al.* 2016).
178 The details of feature table filtering and rarefaction and the parameters invoked in iCAMP and
179 metabolic function prediction pipelines were provided in Supplementary Information **SI-3**.

180 *2.4 Construction of non-redundant metagenome-assembled genomes (MAGs)*

181 The clean paired-end metagenomics reads (~20 Gb/sample) were grouped by sampling periods
182 (season-resolved, **Table S2**) and co-assembled using MEGAHIT v1.13 with default parameters
183 that merge complex bubbles of length $\leq 1 * \text{kmer_size}$ (20) and similarity = 0.95. These co-
184 assembled contigs were clustered to recover draft genomes (v1.3.2, length ≥ 1500 bp) using
185 MaxBin and metaBAT (iterations = 50) as suggested by MetaWRAP (Uritskiy *et al.* 2018). The
186 generated draft genomes were refined to produce high-quality genomic bins using the built-in
187 refining module of MetaWRAP ($> 55\%$ completeness & $< 5\%$ contamination). All bins were
188 further processed with rapid pairwise genome comparisons at a 95% average nucleotide
189 identity (ANI) threshold (Olm *et al.* 2017) to dereplicate the redundant MAGs (alignment
190 fraction $> 10\%$, greedy algorithms). The obtained non-redundant metagenome-assembled
191 genomes (MAGs) were annotated for taxonomic classification (alignment $> 70\%$) using
192 Genome Taxonomy Database (GTDB, v1.4.0) as previously described (Wu *et al.* 2022).

193 *2.5 Identification of intragenomic ARGs and putative pathogenic hosts*

194 The co-assembled scaffolds of all MAGs were initially processed by Prodigal (v2.6.3; -c -p
195 meta mode) to predict open reading frames (ORFs), which was processed by CD-HIT (v4.6, id
196 = 90%, cov = 90%). ABRicate pipelines (v0.9.9; -id 70%, -qcov 75%) were used to detect the
197 human virulent factors and pathogens (vfdb_setB_nt.fas and PATRIC v3.6.12) and ARG
198 marker genes (SARG v2.2) (Arango-Argoty *et al.* 2018, Liu *et al.* 2019a, Wattam *et al.* 2014,
199 Yin *et al.* 2018). An assembled MAG with queried scaffolds showing the coexistence of
200 intragenomic ARGs and virulent/pathogenic marker genes was regarded as the putative
201 resistant pathogen (Liang *et al.* 2019).

202 *2.6 Estimation of HGT potential and community-wide ARGs transfer*

203 The differences in HGT potentials of intragenomic ARGs between putative resistant pathogens
204 and other MAGs were analyzed according to previously published methods with a few
205 modifications (Li *et al.* 2017). In brief, locations of ARGs and MGEs in scaffolds of MAGs
206 were retrieved from the DIAMOND blastx-mode output (alignment =1, -id 70%, -qcov 75%),
207 with respective to the referencing databases of SARG v2.2 and MEGs90 downloaded from the
208 deepARG-DB (Arango-Argoty *et al.* 2020, Buchfink *et al.* 2015). The minimum genetic
209 distance (minDis) pairs of ‘ARGs – MGEs’ in the target genomes were calculated. After that,
210 we randomly selected the bacterial MAGs in three groups including putative pathogenic, non-
211 pathogenic, and all MAGs. This random sampling procedure was repeated 100,000 times. The
212 resulting permutation table of minimum distance pairs with a stepwise increase of genetic
213 distance intervals (increment = 50 bp) was used to calculate the probability of the selected
214 ARGs encountering MGEs (Forsberg *et al.* 2014).

215 All the generated non-redundant ARG-carrying MAGs were applied to MetaCHIP (Song *et al.*

216 2019), which invokes Prodigal generated- ORFs and BLASTx to align and annotate ARGs
217 (alignment to SARG v2.2) and MGEs as suggested (length > 200bp, -id 90%, -qcov 75%,
218 threshold value = 10-e7). The HGT of ‘ARG – MGE’ matching pairs disseminated across the
219 candidate MAGs were predicted via the best-match approach (-BP mode) with taxonomic
220 hierarchy ranks from genus to phylum (-r pcofg). The details of HGT estimation methods and
221 calculating pipelines were provided in Supplementary Information (SI - 3).

222 2.7 Quantification of MAGs and potential hazards

223 The Quant_bin module (default parameters) in the MetaWRAP was used to calculate the
224 relative abundances of constructed MAGs, which were presented in genome copies per million
225 clean sequencing reads (GPMR). The absolute cell counts in the water samples were
226 determined by using a flow cytometer (CytoFLEX, Beckman Coulter, USA), according to the
227 optimized protocols (Nescerecka *et al.* 2016). As suggested by the previous study (Liang *et al.*
228 2019), the cell density of the MAGs (copy/mL-water) in each sample was quantified according
229 to **Eq. 1**, where *Map.r* referred to the percentage of reads in a sample successfully mapped onto
230 the non-redundant MAG reference (BAM files) using Bowtie2 (Langmead and Salzberg 2012);
231 The portion (and number) of reads in each sample’s sequence files generally ranged from 60%
232 to 75% (**Table S2**); *Ab.i* refers to the relative abundance of a target MAG (GPMR); and *i*
233 represented the total number of MAGs.

$$234 \quad \text{MAG. density} = \frac{\text{Absolute cell counts} \times \text{Map.r} \times \text{Ab.i}}{\sum_{i=1}^n \text{Ab.i}} \quad \text{Eq. 1}$$

235 The relative abundance (coverages in the host MAGs) of intragenomic ARGs (ARG-cov/ppm)
236 were calculated according to **Eq. 2**, where *Ab.mag* referred to the relative abundance of the MAG
237 quantified by Quant_bin module (GPMR) and Cov.g denoted the mean coverage of target ARG
238 located on the identified MAGs’ scaffolds; and the mean coverage values of the ARG-

239 associated scaffolds were calculated via built-in pipelines (pileup.sh) of BBmap (v38.87).

240
$$\text{Intra. ARG} = \text{Ab. mag} \times \text{Cov. g} \quad \mathbf{Eq. 2}$$

241 The comparison of overall potential AR risks (a relative-risk index generated) of the resistome
242 among the samples was initially assessed using MetaCompare (Oh *et al.* 2018). The FASTP-
243 filtered clean metagenomic sequences were processed to calculate the abundance and mobility
244 of environmental resistomes and their hosts' pathogenicity with default parameters (10e-10,
245 id >60%, length >150 bp). The details of calculation of MAGs' relative abundances, reads
246 mapping and waterborne cell quantification were provided in Supplementary Information (**SI**
247 **- 2 & SI - 3**).

248 *2.8 Data processing and statistics*

249 The data were log-transformed or scaled to improve sample normality or fitness to specific
250 methods, such as the pairwise t-test and ANOVA test. For datasets that did not fit normal
251 distributions, non-parametric methods were used like Wilcoxon rank-sum test and Kruskal-
252 Wallis rank-sum test. Descriptive analyses of the collected data were performed in Excel 2010
253 (Microsoft Corp. USA), while the advanced statistical analyses (e.g. Mantel test, Procrustes
254 analysis, partitioning of variations, iCAMP-modeling) were performed using *R* 4.0.2
255 (<https://cran.r-project.org/>). The statistical significance was defined at a 95% confidence
256 interval, with a *P*-value of < 0.05 (two-tailed), unless stated otherwise. The details of used
257 statistical methods and installed packages in *R* were explained in detail in Supplementary
258 Information (**SI - 3**).

259 **3. Results and discussion**

260 *3.1 Profile and prevalence of the resistomes across the catchment*

261 The Taipu River originates from Taihu Lake in Jiangsu Province and flows to the Jinze
262 Reservoir in Shanghai (**Fig. 1a**). Along this path, normalized ARG levels in bacterial
263 communities decrease significantly (**Fig. 1b**) from -1.09 ± 0.17 to -1.41 ± 0.08
264 ($\log_{10}(\text{ARGs}/16\text{S rRNA gene})$) based on all samples collected over the study (Two-way
265 ANOVA, $F = 12.1$, $P_{\text{site}} < 0.01$; $P_{\text{season}} = 0.12$). This decreasing trend from upstream to
266 downstream is probably related to the reservoir resettlement (Chen *et al.* 2019) and strict
267 management of the neighboring watershed, where no sewage outfalls and substantially fewer
268 factories are located (**Fig. 1a**). Nevertheless, the mean relative ARG abundances in the Jinze
269 Reservoir resistome was $-1.30 \pm 0.15 \log_{10}(\text{ARGs}/16\text{S rRNA gene})$, which is in the same
270 proportional range as municipal wastewater or activated sludge (**Fig. S1**). Furthermore, the
271 prevalence of specific ARGs is particularly concerning (**Fig. S2**), which encoded resistances to
272 medical antiseptics (*quaE*, $-2.70 \pm 0.18 \log_{10}(\text{ARGs}/16\text{S rRNA gene})$) and frontline antibiotics
273 used in clinical settings (Buffet-Bataillon *et al.* 2012, Petrovich *et al.* 2020), such as
274 carbapenem (*bla_{OXA}*; $-3.05 \pm 0.50 \log_{10}(\text{ARGs}/16\text{S rRNA gene})$), rifamycin (*Arr*; -3.55 ± 0.22
275 $\log_{10}(\text{ARGs}/16\text{S rRNA gene})$), vancomycin (*vanR/S*; $-3.49 \pm 0.30 \log_{10}(\text{ARGs}/16\text{S rRNA}$
276 $\text{gene})$), and polymyxin (*mcr-1/5*; $-4.41 \pm 0.38 \log_{10}(\text{ARGs}/16\text{S rRNA gene})$). These ARGs may
277 stem from the Taipu River's upstream quayside aquaculture farms (**Fig. 1a**), which often
278 misuse antimicrobials and discharge their wastewater along with the water diversion process
279 (Hong *et al.* 2018, Jiang *et al.* 2013, Perry *et al.* 2019, Su and Chen 2020).

280 *3.2 Resistomes determined by microbial assembly and environmental filtering*

281 Resistomes across the catchment were comprised of 103 types of ARGs (**Fig. S2**), which were

282 relatively consistent at our sites during summer and winter sampling (Adonis2, $P > 0.05$, **Fig.**
283 **S3**). The microbial community also exhibited few variations as the Taipu River flowed
284 downstream (Adonis2, $P_{\text{site}} = 0.44$). The observed consistency of site-specific resistomes and
285 microbiomes suggested a close association between ARGs and resident bacteria in the
286 catchment (Procrustes tests, $M^2 = 0.78$, $R = 0.46$, $P = 0.002$, **Fig. S4**).

287 To investigate this relationship from a microbial ecological perspective (Ning *et al.* 2020),
288 season-differentiated microbial assembly processes were simulated (Adonis2, $P_{\text{season}} = 0.01$).
289 As shown in **Fig. 1c**, bacteria in the studied catchment appeared to assemble in a homogeneous
290 selection-dominated approach (HoS, 48% ~ 53%) in both summer and winter samples (ses.cut
291 $= 1.96$, iCAMP), irrespective of variations in geographic locations (One-way ANOVA, $P =$
292 0.17). Among the identified microbial assemblages (**Table S3 & Table S4**), *Microcystis* (26.4%
293 in abundance), *Cyanobiaceae* (10.6%), *Ilumatobacteraceae* (8.9%), and *Burkholderiales* sp.
294 (0.75%) mostly contributed to the HoS process in summer (~ 85%, $\beta\text{NRI} = -2.5$) and winter
295 (~ 90%, $\beta\text{NRI} = -2.2$, **Fig. 1c**). Notably, these assembly-dominant taxa not only exhibited
296 significant correlations to the resistome (Bray-Curtis dissimilarity indices distance, $P < 0.001$,
297 **Fig. 2a**), but also imposed greater impact on ARGs compared with whole microbial taxa
298 (Cohen's $D = 4.22$ vs. 3.39, $P < 0.001$, **Fig. 2a**).

299 The observed high importance (~ 50%) of HoS in the bacterial assembly process ($|\beta\text{NRI}| > 2.0$,
300 **Fig. 1c**) suggests substantial environmental filtering effects on microbial assemblages (Xu *et*
301 *al.* 2020, Yan *et al.* 2016). Here, the forward-selected environmental factors (rda, $\text{AIC} = 278.5$,
302 $P < 0.05$, **Table 1**), including temperature and DO, significantly related to the deterministic
303 assembly of the microbial community ($P < 0.05$, **Fig. 2b**). Decreases in temperature and DO
304 levels (**Table 1**) mirrored microbial responses, especially photoautotrophic processes, such as
305 the oxygenic and photosynthetic pathways of *Cyanobacteria* (LEfSe, $\text{LDA} = 3.0$, $P < 0.01$, **Fig.**

306 **2c & Table S6**). Negative effects of low temperature and DO have been shown for the
307 planktobacteria, including *Microcystis* and *Ilumatobacteraceae* (Mo *et al.* 2018, Zakharova *et*
308 *al.* 2021), which also appear to be resistome-determining taxa in our systems (Cohen's D =
309 4.22, $P < 0.01$, **Fig. 2a**). Environmental filtering and related microbial metabolic responses had
310 a comparable influence to that of assembly-dominant taxa on ARG demographics in the
311 studied catchment (VPA, 12 - 15%, **Table S5**).

312 3.3 Seasonally distributed putative resistant pathogens and intragenomic ARGs

313 There were 266 and 289 non-redundant MAGs obtained from summer and winter samples,
314 respectively, around 20% of which were identified as ARG-hosting bacteria (**Fig. 3**). Overall,
315 these ARG hosts were significantly more abundant across the catchment in summer than in
316 winter (76.8 ± 9.08 vs. 59.0 ± 5.69 GPMR, Pair-wise t-test, $P < 0.01$) and generally belonged
317 to the phyla of *Proteobacteria*, *Bacteroidota* and *Actinobacteria*. Among them, most putative
318 pathogens were *Mycobacteriaceae* (6.83 ± 0.54 GPMR) and *Burkholderiaceae* (19.7 ± 6.51
319 GPMR), of which the distribution and concentrations did not significantly vary across sampling
320 sites (One-way ANOVA, $P > 0.05$; ADONIS, $P = 0.1$, **Fig. S5**). The predominant subtaxon
321 species, such as *M. mycobacterium* spp., and *B. ramibacter* spp. and *Limnohabitans* spp. (**Fig.**
322 **3a**), are frequently associated with human AR infections (Fang *et al.* 2015, Fang *et al.* 2019).
323 In winter samples (**Fig. 3b**), MAGs of putative resistant pathogens were more dispersed across
324 *Actinobacteria* phylum, including *Aeromicrobium*, *Nocardioides*, and *Phycococcus*. These taxa
325 are known to have ill effects on human dermal and intestine health (Singleton *et al.* 2022, Zhang
326 *et al.* 2022). However, the predominant putative resistant pathogens still primarily belonged to
327 *Burkholderiaceae* (12.9 ± 3.83 GPMR) and were evenly distributed across the river (One-way
328 ANOVA, $P > 0.05$).

329 Intragenomic ARGs of putative pathogens were detected with significantly higher diversity

330 and abundance than their counterparts located in other MAGs during the whole period of study
331 (Kruskal-Wallis test, $\chi^2 = 10.6$, $P < 0.01$). In summer samples (**Fig. 3a**), *Burkholderiaceae* and
332 *Mycobacteriaceae* MAGs hosted more than eight types of ARGs, encoding resistance to
333 aminoglycosides, rifamycin, extended-spectrum β -lactams and macrolides ($1.5 - 2.5$
334 $\log_{10}(\text{ARG-cov/ppm})$). In contrast, in winter samples, the predominant constituents of
335 intragenomic resistome were bacitracin ($\sim 2.5 \log_{10}(\text{ARG-cov/ppm})$), rifamycin (~ 1.5
336 $\log_{10}(\text{ARG-cov/ppm})$), and aminoglycoside ($\sim 1.0 \log_{10}(\text{ARG-cov/ppm})$) ARGs (**Fig 3b**), most
337 of which were associated with *Burkholderiaceae* spp., such as *B. limnohabitans* and
338 *Rhizobacter* spp.

339 3.4 Importance of putative pathogens to community-wide HGT of ARG

340 The observed larger and diverse intragenomic ARGs in putative pathogenic bacteria may result
341 from frequent HGT of ARGs (Zhu *et al.* 2013). As shown in **Fig. 4a**, the normalized
342 intragenomic MGE levels, often an approximation of HGT potential (Lamba *et al.* 2017), were
343 significantly correlated with intragenomic ARGs across all samples (Pearson, $P < 0.05$).
344 Importantly, MGEs with apparent links to putative pathogenic MAGs exhibited stronger linear
345 correlations with intragenomic ARGs, suggesting that HGT of ARGs within in situ river
346 microbial communities might be more likely to proceed via resistant pathogenic bacteria
347 (Cohen's D effect size = 0.84 vs. 0.41, $P < 0.001$, **Fig. 4a**). This high HGT potential of ARGs
348 in putative pathogens was seen in both summer and winter samples (Cohen's D effect size >
349 0.6, $P < 0.001$, **Fig. 4a**). Moreover, as shown in **Fig. 4b**, ARGs associated with pathogens had
350 relatively short genetic distance to MGEs on their genetic context contigs (e.g. < 3.5 kb), which
351 is consistent with the previous work that showed greater HGT potential of ARGs in human
352 pathogens compared with overall MAG assemblages (Forsberg *et al.* 2014).

353 The importance of pathogens to dissemination of ARGs was further suggested by a community-

354 wide HGT analysis of all ARG hosting MAGs using the MetaCHIP (Song *et al.* 2019). **Fig 5a**
355 shows that HGT of ARGs more frequently associated with the putative resistant pathogens,
356 irrespective of their roles (i.e. donor vs. recipients) in the HGT processes (Kruskal-Wallis test,
357 $\chi^2 = 17.5$, $P_{path} < 0.001$, $P_{role} = 0.31$). Notably, HGT-involved MAGs primarily belonged to the
358 subtaxa of *Proteobacteria* and *Actinobacteria* (**Fig 5a**), including *Burkholderiaceae* (count =
359 126.8 ± 78.4), *Ilumatobacteraceae* (count = 12.4 ± 6.1) and *Microbacteriaceae* (count = 7.25
360 ± 5.6). These MAGs not only exhibited more frequent ARG transmission (Kruskal-Wallis test,
361 $\chi^2 = 96.3$, $P < 0.001$), but also were identified as the microbial assembly-dominant taxa that
362 shaped the resistomes (**Fig. 2a & Table S4**).

363 Although *Cyanobacteria* dominated microbial assembly and resistome variations, evidence
364 suggests they were not closely involved in the community-wide ARG HGT (count < 3.0, **Fig**
365 **5a**) and their acquired intragenomic ARGs all originated from putative pathogenic MAGs of
366 *Burkholderiaceae* sp. (**Fig. S7 & Fig. S8**) with high HGT potentials (**Fig. 5a**). From the
367 microbial synergistic perspective, *Burkholderiaceae* can utilize algal excrements (e.g.
368 microcystin) as major metabolic substrates (Salter et al. 2021), therefore the cyanobacterial
369 aggregates tend to closely structure with *Burkholderiaceae* in lake-river ecosystems (Eiler and
370 Bertilsson 2004) . As reported by Guo et al. (2018), waterborne ARGs and their hosting
371 bacteria were abundantly observed in the bacterioplanktonic aggregates. In the homogeneous
372 selection dominated community (**Fig. 1**), *Cyanobacteria* exhibit high resiliance to
373 environmental variations (Liu et al. 2019b, Mo et al. 2018), which could be beneficial to
374 preserve their associated ARGs (**Fig. 5**). The predominant intragenomic ARGs, including β -
375 lactam resistant (e.g. *bla*_{OXA}) and MLS resistant genes (*macB*), appeared to be disseminated
376 between microbial assembly-dominant taxa and putative resistant pathogens (**Fig. 5b**), which
377 explains the high prevalence and the spread of ARGs across the catchment during the period
378 of water diversion.

379 3.5 Implications of potential AR hazards and influencing factors

380 The prevalence of ARGs with potential clinical importance (**Fig. 1c** & **Fig. S2**) and putative
381 resistant pathogens (**Fig. 3**) may suggest higher AR risks (Martinez *et al.* 2015), especially if
382 they are found in drinking water sources (Dang *et al.* 2020, Walsh *et al.* 2011). Overall, summer
383 samples showed higher potential AR hazards using MetaCompare (index values = 19.3 *vs.*
384 19.0). The potential exposure risks were significantly lower in the reservoir *vs.* upstream (Two-
385 way ANOVA, $P < 0.05$, **Fig. S8**). This trend was mirrored by lower density of putative resistant
386 pathogens in the reservoir water samples, *i.e.* $3.79 \pm 2.5 \times 10^6$ cell/L on average (One-way
387 ANOVA, $F = 31.4$, $P < 0.001$, **Fig. 6a**). This value corresponds to a total amount of 13.3 ± 0.89
388 $\times 10^{15}$ cells of putative resistant pathogens that are transferred daily to Shanghai's water supply
389 system during the water diversion process (3.5 million m³/day). However, it should be noted
390 that this study was confined to just one catchment. For better generalization of at-tap drinking
391 water source-specific AR, a combination of metagenomics and culture-based studies that
392 comprehensively encompass water sources, distribution networks and household tap water at
393 a national or continental scale is needed.

394 A more in-depth analysis using structural equation modelling (SEM) revealed direct effects
395 concerning the distribution of resistome (std-coeff $\beta = 0.69$, $P < 0.05$) and microbial assembly-
396 dominant bacteria (std-coeff $\beta = 0.15$, $P < 0.05$) on the absolute concentration of waterborne
397 putative resistant pathogens across the studied catchment (**Fig. 6b**). Nevertheless, the
398 environmental filtering factors including temperature and DO values (SEM, std-coeff $|\beta| \geq 0.8$,
399 $P < 0.05$), only showed indirect effects via their influence on the microbial assembly-dominant
400 bacterial taxa (SEM, std-coeff $\beta = -0.45$, $P < 0.05$). This suggests that improvement of water
401 quality may have a limited effect on reducing in-situ resistome transmission and resistant
402 pathogens ($P > 0.05$, **Fig. 6b**), whereas the holistic management of wastewater inputs

403 containing pathogens (Jiang *et al.* 2013, Quintela-Baluja *et al.* 2019) and control of microbial
404 assembly-dominant bacterial taxa, such as curbing algal (*e.g.* *Cyanobacteria*) blooms are
405 critically needed (Guo *et al.* 2018, Mo *et al.* 2018, Xue *et al.* 2018).

406 **4. Conclusions**

407 Here, we show that microbial deterministic assembly process is critical to the resulting
408 environmental antibiotic resistomes in the Taipu River catchment. The seasonal variations of
409 ARGs, including the ones of particular importance to human health, were frequently hosted by
410 putative pathogenic bacteria, which greatly contributed to the community-wide HGT of ARGs,
411 especially with the assembly-dominant taxa.

412 The pipelines constructed to estimate ARGs' HGT potentials can be applied more generally in
413 a wide range of environmental settings, for quantitative comparison and analysis of resistome
414 mobility and potential AR risks. Importantly, in the annually operated water diversion process
415 in the Taihu Basin, the waterborne ARGs released from upstream sources are 'well-preserved'
416 in the niched bacterial community and transferred to the downstream drinking water reservoir,
417 which presumably contains $3.0 \sim 4.0 \times 10^6$ cell/L of the putative resistant pathogens. Although
418 our data are from samples prior to water treatment, there is an implicit concern about AR spread
419 through the local water supply, possibly impacting 24 million Shanghai citizens. However, the
420 work also shows importance of environmental factors and microbial spatial ecology on ARG
421 fate, which provides a useful starting point for developing strategies to curb the AR
422 transmission in the Shanghai or other water supply catchments.

423 **CRedit Authorship Contribution Statement**

424 K.Y. and B.X. designed and obtained funding for this study; D.W., Y-L.S., and J.Z. collected

425 samples and raw sequencing data and conducted the experiments; D.W., J.Z., and M-J. Y.
426 undertook the bioinformatics analyses and contributed to the data visualization. D.W., D.W.G.
427 Y-L.S., J.D., and B.X. wrote the paper. All of the authors read and approved the final
428 manuscript.

429 **Declaration of Competing Interest**

430 The authors declare that they have no known competing financial interests or personal
431 relationships that could have appeared to influence the work reported in this paper.

432 **Acknowledgments**

433 This work was financially supported by the National Key Research and Development Program
434 of China (2018YFC1901000), Major Science and Technology Program for Water Pollution
435 Control and Treatment (2017ZX07207003-01), National Natural Science Foundation of China
436 (42107457 and 22276059), Key Laboratory of Environmental Pollution Monitoring and
437 Disease Control, Ministry of Education, Guizhou Medical University (KY2022383).
438 Guangdong-Hong Kong-Macao Joint Laboratory for Contaminants Exposure and Health,
439 Guangdong University of Technology (GHMJLCEH-12). The authors thank Editor, Reviewers,
440 and Prof. Tong Zhang and his team from the University of Hong Kong for their suggestions
441 and comments to improve the quality of the manuscript.

442 **Supplementary Materials**

443 The Supplementary Information (SI) is available free of charge on the Elsevier Publication
444 Water Research website (<https://www.journals.elsevier.com/water-research>). The provided SI
445 was comprised of four sections including sampling and pretreatment information (**SI-1**), details
446 of utilized microbial molecular techniques (**SI-2**), bioinformatics methods and related

447 calculations (**SI-3**), and supplementary analyzing results (**SI-4**).

448 **References**

- 449 Amos, G.C.A., Ploumaki, S., Zhang, L., Hawkey, P.M., Gaze, W.H. and Wellington, E.M.H.
450 (2018) The Widespread Dissemination of Integrons Throughout Bacterial Communities in a
451 Riverine System. *ISME J* 12(3), 681-691. doi:10.1038/s41396-017-0030-8
- 452 Arango-Argoty, G., Garner, E., Pruden, A., Heath, L.S., Vikesland, P. and Zhang, L. (2018)
453 Deeparg: A Deep Learning Approach for Predicting Antibiotic Resistance Genes from
454 Metagenomic Data. *Microbiome* 6(1), 23. doi:10.1186/s40168-018-0401-z
- 455 Arango-Argoty, G.A., Guron, G.K.P., Garner, E., Riquelme, M.V., Heath, L.S., Pruden, A.,
456 Vikesland, P.J. and Zhang, L. (2020) Argminer: A Web Platform for the Crowdsourcing-Based
457 Curation of Antibiotic Resistance Genes. *Bioinformatics* 36(9), 2966-2973.
458 doi:10.1093/bioinformatics/btaa095
- 459 Buchfink, B., Xie, C. and Huson, D.H. (2015) Fast and Sensitive Protein Alignment Using
460 Diamond. *Nature Methods* 12(1), 59-60. doi:DOI 10.1038/nmeth.3176
- 461 Buffet-Bataillon, S., Tattevin, P., Bonnaure-Mallet, M. and Jolivet-Gougeon, A. (2012)
462 Emergence of Resistance to Antibacterial Agents: The Role of Quaternary Ammonium
463 Compounds--a Critical Review. *Int J Antimicrob Agents* 39(5), 381-389.
464 doi:10.1016/j.ijantimicag.2012.01.011
- 465 Chen, H., Li, Y., Sun, W., Song, L., Zuo, R. and Teng, Y. (2020) Characterization and Source
466 Identification of Antibiotic Resistance Genes in the Sediments of an Interconnected River-Lake
467 System. *Environment International* 137, 105538. doi:10.1016/j.envint.2020.105538
- 468 Chen, Y., Su, J.Q., Zhang, J., Li, P., Chen, H., Zhang, B., Gin, K.Y. and He, Y. (2019) High-
469 Throughput Profiling of Antibiotic Resistance Gene Dynamic in a Drinking Water River-
470 Reservoir System. *Water Res* 149, 179-189. doi:10.1016/j.watres.2018.11.007
- 471 D'Costa, V.M., King, C.E., Kalan, L., Morar, M., Sung, W.W., Schwarz, C., Froese, D., Zazula,
472 G., Calmels, F., Debruyne, R., Golding, G.B., Poinar, H.N. and Wright, G.D. (2011) Antibiotic
473 Resistance Is Ancient. *Nature* 477(7365), 457-461. doi:10.1038/nature10388
- 474 D'Costa, V.M., McGrann, K.M., Hughes, D.W. and Wright, G.D. (2006) Sampling the
475 Antibiotic Resistome. *Science* 311(5759), 374-377. doi:10.1126/science.1120800
- 476 Dang, C., Xia, Y., Zheng, M., Liu, T., Liu, W., Chen, Q. and Ni, J. (2020) Metagenomic Insights
477 into the Profile of Antibiotic Resistomes in a Large Drinking Water Reservoir. *Environment*
478 *International* 136, 105449. doi:10.1016/j.envint.2019.105449
- 479 Eiler, A. and Bertilsson, S. (2004) Composition of Freshwater Bacterial Communities
480 Associated with Cyanobacterial Blooms in Four Swedish Lakes. *Environ Microbiol* 6(12),
481 1228-1243. doi:10.1111/j.1462-2920.2004.00657.x
- 482 Elder, F.C.T., Proctor, K., Barden, R., Gaze, W.H., Snape, J., Feil, E.J. and Kasprzyk-Hordern,
483 B. (2021) Spatiotemporal Profiling of Antibiotics and Resistance Genes in a River Catchment:
484 Human Population as the Main Driver of Antibiotic and Antibiotic Resistance Gene Presence

485 in the Environment. *Water Res* 203, 117533. doi:10.1016/j.watres.2021.117533

486 Fang, H., Wang, H., Cai, L. and Yu, Y. (2015) Prevalence of Antibiotic Resistance Genes and
487 Bacterial Pathogens in Long-Term Manured Greenhouse Soils as Revealed by Metagenomic
488 Survey. *Environ Sci Technol* 49(2), 1095-1104. doi:10.1021/es504157v

489 Fang, P., Peng, F., Gao, X., Xiao, P. and Yang, J. (2019) Decoupling the Dynamics of Bacterial
490 Taxonomy and Antibiotic Resistance Function in a Subtropical Urban Reservoir as Revealed
491 by High-Frequency Sampling. *Front Microbiol* 10, 1448. doi:10.3389/fmicb.2019.01448

492 Forsberg, K.J., Patel, S., Gibson, M.K., Lauber, C.L., Knight, R., Fierer, N. and Dantas, G.
493 (2014) Bacterial Phylogeny Structures Soil Resistomes across Habitats. *Nature* 509(7502),
494 612-616. doi:10.1038/nature13377

495 Forsberg, K.J., Reyes, A., Wang, B., Selleck, E.M., Sommer, M.O. and Dantas, G. (2012) The
496 Shared Antibiotic Resistome of Soil Bacteria and Human Pathogens. *Science* 337(6098), 1107-
497 1111. doi:10.1126/science.1220761

498 Gibson, M.K., Forsberg, K.J. and Dantas, G. (2015) Improved Annotation of Antibiotic
499 Resistance Determinants Reveals Microbial Resistomes Cluster by Ecology. *ISME J* 9(1), 207-
500 216. doi:10.1038/ismej.2014.106

501 Guo, Y., Liu, M., Liu, L., Liu, X., Chen, H. and Yang, J. (2018) The Antibiotic Resistome of
502 Free-Living and Particle-Attached Bacteria under a Reservoir Cyanobacterial Bloom. *Environ*
503 *Int* 117, 107-115. doi:10.1016/j.envint.2018.04.045

504 Hassan, B., Ijaz, M., Khan, A., Sands, K., Serfas, G.I., Clayfield, L., El-Bouseary, M.M., Lai,
505 G., Portal, E., Khan, A., Watkins, W.J., Parkhill, J. and Walsh, T.R. (2021) A Role for
506 Arthropods as Vectors of Multidrug-Resistant Enterobacterales in Surgical Site Infections from
507 South Asia. *Nat Microbiol* 6(10), 1259-1270. doi:10.1038/s41564-021-00965-1

508 Jiang, L., Hu, X., Xu, T., Zhang, H., Sheng, D. and Yin, D. (2013) Prevalence of Antibiotic
509 Resistance Genes and Their Relationship with Antibiotics in the Huangpu River and the
510 Drinking Water Sources, Shanghai, China. *Sci Total Environ* 458-460, 267-272.
511 doi:10.1016/j.scitotenv.2013.04.038

512 Lamba, M., Graham, D.W. and Ahammad, S.Z. (2017) Hospital Wastewater Releases of
513 Carbapenem-Resistance Pathogens and Genes in Urban India. *Environ Sci Technol* 51(23),
514 13906-13912. doi:10.1021/acs.est.7b03380

515 Langmead, B. and Salzberg, S.L. (2012) Fast Gapped-Read Alignment with Bowtie 2. *Nature*
516 *Methods* 9(4), 357-359. doi:10.1038/nmeth.1923

517 Larsson, D.G.J., Andremon, A., Bengtsson-Palme, J., Brandt, K.K., de Roda Husman, A.M.,
518 Fagerstedt, P., Fick, J., Flach, C.F., Gaze, W.H., Kuroda, M., Kvint, K., Laxminarayan, R.,
519 Manaia, C.M., Nielsen, K.M., Plant, L., Ploy, M.C., Segovia, C., Simonet, P., Smalla, K., Snape,
520 J., Topp, E., van Hengel, A.J., Verner-Jeffreys, D.W., Virta, M.P.J., Wellington, E.M. and
521 Wernersson, A.S. (2018) Critical Knowledge Gaps and Research Needs Related to the
522 Environmental Dimensions of Antibiotic Resistance. *Environment International* 117, 132-138.
523 doi:10.1016/j.envint.2018.04.041

- 524 Li, L.G., Xia, Y. and Zhang, T. (2017) Co-Occurrence of Antibiotic and Metal Resistance
525 Genes Revealed in Complete Genome Collection. *ISME J* 11(3), 651–662.
526 doi:10.1038/ismej.2016.155
- 527 Liang, J., Mao, G., Yin, X., Ma, L., Liu, L., Bai, Y., Zhang, T. and Qu, J. (2019) Identification
528 and Quantification of Bacterial Genomes Carrying Antibiotic Resistance Genes and Virulence
529 Factor Genes for Aquatic Microbiological Risk Assessment. *Water Res* 168, 115160.
530 doi:10.1016/j.watres.2019.115160
- 531 Liu, B., Zheng, D., Jin, Q., Chen, L. and Yang, J. (2019a) Vfdb 2019: A Comparative
532 Pathogenomic Platform with an Interactive Web Interface. *Nucleic Acids Res* 47(D1), D687-
533 D692. doi:10.1093/nar/gky1080
- 534 Liu, L., Chen, H., Liu, M., Yang, J.R., Xiao, P., Wilkinson, D.M. and Yang, J. (2019b) Response
535 of the Eukaryotic Plankton Community to the Cyanobacterial Biomass Cycle over 6 Years in
536 Two Subtropical Reservoirs. *ISME J* 13(9), 2196-2208. doi:10.1038/s41396-019-0417-9
- 537 Louca, S., Parfrey, L.W. and Doebeli, M. (2016) Decoupling Function and Taxonomy in the
538 Global Ocean Microbiome. *Science* 353(6305), 1272-1277. doi:10.1126/science.aaf4507
- 539 Maavara, T., Lauerwald, R., Regnier, P. and Van Cappellen, P. (2017) Global Perturbation of
540 Organic Carbon Cycling by River Damming. *Nat Commun* 8, 15347.
541 doi:10.1038/ncomms15347
- 542 Mahnert, A., Moissl-Eichinger, C., Zojer, M., Bogumil, D., Mizrahi, I., Rattei, T., Martinez,
543 J.L. and Berg, G. (2019) Man-Made Microbial Resistances in Built Environments. *Nat*
544 *Commun* 10(1), 968. doi:10.1038/s41467-019-08864-0
- 545 Martinez, J.L., Coque, T.M. and Baquero, F. (2015) What Is a Resistance Gene? Ranking Risk
546 in Resistomes. *Nat Rev Microbiol* 13(2), 116-123. doi:10.1038/nrmicro3399
- 547 McCann, C.M., Christgen, B., Roberts, J.A., Su, J.Q., Arnold, K.E., Gray, N.D., Zhu, Y.G. and
548 Graham, D.W. (2019) Understanding Drivers of Antibiotic Resistance Genes in High Arctic
549 Soil Ecosystems. *Environment International* 125, 497-504. doi:10.1016/j.envint.2019.01.034
- 550 Mo, Y., Zhang, W., Yang, J., Lin, Y., Yu, Z. and Lin, S. (2018) Biogeographic Patterns of
551 Abundant and Rare Bacterioplankton in Three Subtropical Bays Resulting from Selective and
552 Neutral Processes. *ISME J* 12(9), 2198-2210. doi:10.1038/s41396-018-0153-6
- 553 Munck, C., Albertsen, M., Telke, A., Ellabaan, M., Nielsen, P.H. and Sommer, M.O. (2015)
554 Limited Dissemination of the Wastewater Treatment Plant Core Resistome. *Nat Commun* 6,
555 8452. doi:10.1038/ncomms9452
- 556 Nescerecka, A., Hammes, F. and Juhna, T. (2016) A Pipeline for Developing and Testing
557 Staining Protocols for Flow Cytometry, Demonstrated with Sybr Green I and Propidium Iodide
558 Viability Staining. *Journal of Microbiological Methods* 131, 172-180.
559 doi:10.1016/j.mimet.2016.10.022
- 560 Ning, D., Yuan, M., Wu, L., Zhang, Y., Guo, X., Zhou, X., Yang, Y., Arkin, A.P., Firestone,
561 M.K. and Zhou, J. (2020) A Quantitative Framework Reveals Ecological Drivers of Grassland

- 562 Microbial Community Assembly in Response to Warming. *Nat Commun* 11(1), 4717.
563 doi:10.1038/s41467-020-18560-z
- 564 Oh, M., Pruden, A., Chen, C., Heath, L.S., Xia, K. and Zhang, L. (2018) Metacompare: A
565 Computational Pipeline for Prioritizing Environmental Resistome Risk. *FEMS Microbiol Ecol*
566 94(7), fiy079. doi:10.1093/femsec/fiy079
- 567 Olm, M.R., Brown, C.T., Brooks, B. and Banfield, J.F. (2017) Drep: A Tool for Fast and
568 Accurate Genomic Comparisons That Enables Improved Genome Recovery from
569 Metagenomes through De-Replication. *ISME J* 11(12), 2864-2868.
570 doi:10.1038/ismej.2017.126
- 571 Pehrsson, E.C., Tsukayama, P., Patel, S., Mejia-Bautista, M., Sosa-Soto, G., Navarrete, K.M.,
572 Calderon, M., Cabrera, L., Hoyos-Arango, W., Bertoli, M.T., Berg, D.E., Gilman, R.H. and
573 Dantas, G. (2016) Interconnected Microbiomes and Resistomes in Low-Income Human
574 Habitats. *Nature* 533(7602), 212-216. doi:10.1038/nature17672
- 575 Petrovich, M.L., Zilberman, A., Kaplan, A., Eliraz, G.R., Wang, Y., Langenfeld, K., Duhaime,
576 M., Wigginton, K., Poretsky, R., Avisar, D. and Wells, G.F. (2020) Microbial and Viral
577 Communities and Their Antibiotic Resistance Genes Throughout a Hospital Wastewater
578 Treatment System. *Front Microbiol* 11, 153. doi:10.3389/fmicb.2020.00153
- 579 Quintela-Baluja, M., Abouelnaga, M., Romalde, J., Su, J.Q., Yu, Y., Gomez-Lopez, M., Smets,
580 B., Zhu, Y.G. and Graham, D.W. (2019) Spatial Ecology of a Wastewater Network Defines the
581 Antibiotic Resistance Genes in Downstream Receiving Waters. *Water Res* 162, 347-357.
582 doi:10.1016/j.watres.2019.06.075
- 583 Quintela-Baluja, M., Frigon, D., Abouelnaga, M., Jobling, K., Romalde, J.L., Gomez Lopez,
584 M. and Graham, D.W. (2021) Dynamics of Integron Structures across a Wastewater Network -
585 Implications to Resistance Gene Transfer. *Water Res* 206, 117720.
586 doi:10.1016/j.watres.2021.117720
- 587 Rysz, M., Mansfield, W.R., Fortner, J.D. and Alvarez, P.J. (2013) Tetracycline Resistance Gene
588 Maintenance under Varying Bacterial Growth Rate, Substrate and Oxygen Availability, and
589 Tetracycline Concentration. *Environ Sci Technol* 47(13), 6995-7001. doi:10.1021/es3035329
- 590 Salter, C., VanMensel, D., Reid, T., Birbeck, J., Westrick, J., Mundle, S.O.C. and Weisener,
591 C.G. (2021) Investigating the Microbial Dynamics of Microcystin-Lr Degradation in Lake Erie
592 Sand. *Chemosphere* 272, 129873. doi:10.1016/j.chemosphere.2021.129873
- 593 Singleton, C.M., Petriglieri, F., Wasmund, K., Nierychlo, M., Kondrotaitė, Z., Petersen, J.F.,
594 Peces, M., Dueholm, M.S., Wagner, M. and Nielsen, P.H. (2022) The Novel Genus, 'Candidatus
595 Phosphoribacter', Previously Identified as *Tetrasphaera*, Is the Dominant Polyphosphate
596 Accumulating Lineage in Ebpr Wastewater Treatment Plants Worldwide. *ISME J*.
597 doi:10.1038/s41396-022-01212-z
- 598 Smillie, C.S., Smith, M.B., Friedman, J., Cordero, O.X., David, L.A. and Alm, E.J. (2011)
599 Ecology Drives a Global Network of Gene Exchange Connecting the Human Microbiome.
600 *Nature* 480(7376), 241-244. doi:10.1038/nature10571

- 601 Song, W., Wemheuer, B., Zhang, S., Steensen, K. and Thomas, T. (2019) Metachip:
602 Community-Level Horizontal Gene Transfer Identification through the Combination of Best-
603 Match and Phylogenetic Approaches. *Microbiome* 7(1), 36. doi:10.1186/s40168-019-0649-y
- 604 Su, J.Q., Wei, B., Ou-Yang, W.Y., Huang, F.Y., Zhao, Y., Xu, H.J. and Zhu, Y.G. (2015)
605 Antibiotic Resistome and Its Association with Bacterial Communities During Sewage Sludge
606 Composting. *Environ Sci Technol* 49(12), 7356-7363. doi:10.1021/acs.est.5b01012
- 607 Sun, J., Liao, X.P., D'Souza, A.W., Boolchandani, M., Li, S.H., Cheng, K., Luis Martinez, J.,
608 Li, L., Feng, Y.J., Fang, L.X., Huang, T., Xia, J., Yu, Y., Zhou, Y.F., Sun, Y.X., Deng, X.B.,
609 Zeng, Z.L., Jiang, H.X., Fang, B.H., Tang, Y.Z., Lian, X.L., Zhang, R.M., Fang, Z.W., Yan,
610 Q.L., Dantas, G. and Liu, Y.H. (2020) Environmental Remodeling of Human Gut Microbiota
611 and Antibiotic Resistome in Livestock Farms. *Nat Commun* 11(1), 1427. doi:10.1038/s41467-
612 020-15222-y
- 613 Tan, L., Wang, F., Liang, M., Wang, X., Das, R., Mao, D. and Luo, Y. (2019) Antibiotic
614 Resistance Genes Attenuated with Salt Accumulation in Saline Soil. *J Hazard Mater* 374, 35-
615 42. doi:10.1016/j.jhazmat.2019.04.020
- 616 Uritskiy, G.V., DiRuggiero, J. and Taylor, J. (2018) Metawrap-a Flexible Pipeline for Genome-
617 Resolved Metagenomic Data Analysis. *Microbiome* 6(1), 158. doi:10.1186/s40168-018-0541-
618 1
- 619 Walsh, T.R., Weeks, J., Livermore, D.M. and Toleman, M.A. (2011) Dissemination of Ndm-1
620 Positive Bacteria in the New Delhi Environment and Its Implications for Human Health: An
621 Environmental Point Prevalence Study. *Lancet Infect Dis* 11(5), 355-362. doi:10.1016/s1473-
622 3099(11)70059-7
- 623 Wang, J., Qin, X., Guo, J., Jia, W., Wang, Q., Zhang, M. and Huang, Y. (2020) Evidence of
624 Selective Enrichment of Bacterial Assemblages and Antibiotic Resistant Genes by
625 Microplastics in Urban Rivers. *Water Res* 183, 116113. doi:10.1016/j.watres.2020.116113
- 626 Wattam, A.R., Abraham, D., Dalay, O., Disz, T.L., Driscoll, T., Gabbard, J.L., Gillespie, J.J.,
627 Gough, R., Hix, D., Kenyon, R., Machi, D., Mao, C., Nordberg, E.K., Olson, R., Overbeek, R.,
628 Pusch, G.D., Shukla, M., Schulman, J., Stevens, R.L., Sullivan, D.E., Vonstein, V., Warren, A.,
629 Will, R., Wilson, M.J., Yoo, H.S., Zhang, C., Zhang, Y. and Sobral, B.W. (2014) Patric, the
630 Bacterial Bioinformatics Database and Analysis Resource. *Nucleic Acids Res* 42(Database
631 issue), D581-591. doi:10.1093/nar/gkt1099
- 632 Winter, M., Buckling, A., Harms, K., Johnsen, P.J. and Vos, M. (2021) Antimicrobial
633 Resistance Acquisition Via Natural Transformation: Context Is Everything. *Current Opinion in*
634 *Microbiology* 64, 133-138. doi:10.1016/j.mib.2021.09.009
- 635 Wu, D., Jin, L., Xie, J., Liu, H., Zhao, J., Ye, D. and Li, X.-d. (2022) Inhalable Antibiotic
636 Resistomes Emitted from Hospitals: Metagenomic Insights into Bacterial Hosts, Clinical
637 Relevance, and Environmental Risks. *Microbiome* 10(1), in press. doi:10.1186/s40168-021-
638 01197-5
- 639 Wu, D., Su, Y., Xi, H., Chen, X. and Xie, B. (2019) Urban and Agriculturally Influenced Water
640 Contribute Differently to the Spread of Antibiotic Resistance Genes in a Mega-City River

- 641 Network. *Water Res* 158, 11-21. doi:10.1016/j.watres.2019.03.010
- 642 Xie, J., Jin, L., He, T., Chen, B., Luo, X., Feng, B., Huang, W., Li, J., Fu, P. and Li, X. (2019)
643 Bacteria and Antibiotic Resistance Genes (Args) in Pm2.5 from China: Implications for Human
644 Exposure. *Environ Sci Technol* 53(2), 963-972. doi:10.1021/acs.est.8b04630
- 645 Xu, X., Wang, N., Lipson, D., Sinsabaugh, R., Schimel, J., He, L., Soudzilovskaia, N.A.,
646 Tedersoo, L. and Algar, A.C. (2020) Microbial Macroecology: In Search of Mechanisms
647 Governing Microbial Biogeographic Patterns. *Global Ecology and Biogeography* 29(11),
648 1870-1886. doi:10.1111/geb.13162
- 649 Xue, Y., Chen, H., Yang, J.R., Liu, M., Huang, B. and Yang, J. (2018) Distinct Patterns and
650 Processes of Abundant and Rare Eukaryotic Plankton Communities Following a Reservoir
651 Cyanobacterial Bloom. *ISME J* 12(9), 2263-2277. doi:10.1038/s41396-018-0159-0
- 652 Yan, Q., Li, J., Yu, Y., Wang, J., He, Z., Van Nostrand, J.D., Kempfer, M.L., Wu, L., Wang, Y.,
653 Liao, L., Li, X., Wu, S., Ni, J., Wang, C. and Zhou, J. (2016) Environmental Filtering Decreases
654 with Fish Development for the Assembly of Gut Microbiota. *Environmental Microbiology*
655 18(12), 4739-4754. doi:10.1111/1462-2920.13365
- 656 Yang, Y., Jiang, X.T., Chai, B.L., Ma, L.P., Li, B., Zhang, A.N., Cole, J.R., Tiedje, J.M. and
657 Zhang, T. (2016) Args-Oap: Online Analysis Pipeline for Antibiotic Resistance Genes
658 Detection from Metagenomic Data Using an Integrated Structured Arg-Database.
659 *Bioinformatics* 32(15), 2346-2351. doi:10.1093/bioinformatics/btw136
- 660 Yin, X., Jiang, X.T., Chai, B., Li, L., Yang, Y., Cole, J.R., Tiedje, J.M. and Zhang, T. (2018)
661 Args-Oap V2.0 with an Expanded Sarg Database and Hidden Markov Models for Enhancement
662 Characterization and Quantification of Antibiotic Resistance Genes in Environmental
663 Metagenomes. *Bioinformatics* 34(13), 2263-2270. doi:10.1093/bioinformatics/bty053
- 664 Zakharova, Y., Bashenkhayeva, M., Galachyants, Y., Petrova, D., Tomberg, I., Marchenkov, A.,
665 Kopyrina, L. and Likhoshway, Y. (2021) Variability of Microbial Communities in Two Long-
666 Term Ice-Covered Freshwater Lakes in the Subarctic Region of Yakutia, Russia. *Microb Ecol.*
667 doi:10.1007/s00248-021-01912-7
- 668 Zhang, Y., Chen, J., Chen, H., Liu, L., Liu, C. and Teng, Y. (2022) An Integrated
669 Multidisciplinary-Based Framework for Characterizing Environmental Risks of Heavy Metals
670 and Their Effects on Antibiotic Resistomes in Agricultural Soils. *J Hazard Mater* 426, 128113.
671 doi:10.1016/j.jhazmat.2021.128113
- 672 Zhu, G., Wang, X., Yang, T., Su, J., Qin, Y., Wang, S., Gillings, M., Wang, C., Ju, F., Lan, B.,
673 Liu, C., Li, H., Long, X.E., Wang, X., Jetten, M.S.M., Wang, Z. and Zhu, Y.G. (2021) Air
674 Pollution Could Drive Global Dissemination of Antibiotic Resistance Genes. *ISME J* 15(1),
675 270-281. doi:10.1038/s41396-020-00780-2
- 676 Zhu, Y.G., Johnson, T.A., Su, J.Q., Qiao, M., Guo, G.X., Stedtfeld, R.D., Hashsham, S.A. and
677 Tiedje, J.M. (2013) Diverse and Abundant Antibiotic Resistance Genes in Chinese Swine
678 Farms. *Proc Natl Acad Sci U S A* 110(9), 3435-3440. doi:10.1073/pnas.1222743110
- 679 Zhu, Y.G., Zhao, Y., Li, B., Huang, C.L., Zhang, S.Y., Yu, S., Chen, Y.S., Zhang, T., Gillings,

680 M.R. and Su, J.Q. (2017) Continental-Scale Pollution of Estuaries with Antibiotic Resistance
681 Genes. *Nat Microbiol* 2, 16270. doi:10.1038/nmicrobiol.2016.270

682

Declaration of interests

The authors declare that they have no known competing financial interests or personal relationships that could have appeared to influence the work reported in this paper.

The authors declare the following financial interests/personal relationships which may be considered as potential competing interests:

Dong Wu reports financial support was provided by National Natural Science Foundation of China. Dong Wu reports financial support was provided by Key Laboratory of Environmental Pollution Monitoring and Disease Control, Ministry of Education. Dong Wu reports financial support was provided by Guangdong-Hong Kong-Macao Joint Laboratory for Contaminants Exposure and Health. Bing Xie, Kai Yang reports financial support was provided by National Key Research and Development Program of China. Bing Xie reports financial support was provided by National Natural Science Foundation of China.

Table 1 Measurement and forward-selection of physiochemical parameters of water samples in Taipu Catchment

#Forward-selected factors	TP ¹		PW ²		LL ²		LX ²		JZi ³		JZe ³	
	(Summer Winter)	(Summer Winter)	(Summer Winter)	(Summer Winter)	(Summer Winter)	(Summer Winter)	(Summer Winter)	(Summer Winter)	(Summer Winter)	(Summer Winter)	(Summer Winter)	(Summer Winter)
TN (sd)	1.56	1.55	1.81	1.39	1.66	1.37	1.71	1.37	1.17	0.80	1.01	1.36
<i>0.1 > P > 0.05</i>	(0.03)	(0.20)	(1.01)	(0.15)	(0.21)	(0.29)	(0.16)	(0.3)	(0.28)	(0.17)	(0.16)	(0.11)
Nitrate-N (sd)	0.67	0.63	0.73	0.62	0.57	0.50	0.75	0.62	0.58	0.22	0.25	0.12
<i>0.1 > P > 0.05</i>	(0.11)	(0.06)	(0.60)	(0.08)	(0.09)	(0.14)	(0.19)	(0.11)	(0.27)	(0.15)	(0.15)	(0.08)
Ammonium-N (sd)	1.01	0.98	1.10	0.89	0.87	0.91	1.11	0.58	0.51	0.77	0.71	1.21
<i>0.1 > P > 0.05</i>	(0.13)	(0.10)	(0.71)	(0.25)	(0.11)	(0.21)	(0.06)	(0.18)	(0.31)	(0.23)	(0.14)	(0.10)
DO (sd)	6.3	5.5	7.2	4.81	6.21	5.03	5.40	4.03	6.41	5.05	6.30	5.82
<i>P = 0.01; AIC = 201.6</i>	(0.90)	(0.70)	(1.82)	(1.59)	(2.03)	(1.06)	(0.55)	(1.85)	(1.83)	(0.44)	(1.09)	(1.17)
Temperature (sd)	22.5	14.6	21.4	13.3	21.8	12.6	23.3	11.6	20.7	10.8	21.7	11.7
<i>P = 0.04; AIC = 201.7</i>	(5.20)	(2.47)	(1.82)	(5.68)	(1.78)	(5.73)	(2.02)	(5.89)	(1.50)	(5.53)	(1.71)	(5.97)
*FCs (sd)	6.23	5.20	2.05	7.12	2.57	2.07	2.36	10.0	5.00	6.35	5.70	6.25
<i>0.1 > P > 0.05</i>	(4.43)	(3.56)	(1.71)	(7.05)	(1.97)	(1.48)	(1.87)	(8.52)	(2.49)	(1.71)	(3.76)	(2.55)
Flowrate (sd)	112.85	81.80	154.28	149.06	236.20	230.33	289.73	280.58	123.97	148.36	216.92	158.61
<i>P = 0.05; AIC = 204.5</i>	(18.7)	(1.70)	(35.1)	(22.7)	(58.6)	(13.1)	(13.3)	(47.6)	(61.2)	(26.5)	(33.6)	(64.4)

¹ TP water was sampled from the effluents from Taihu Lake pumping stations; ² PW, LL, and LX river were sampled from the middle of Taipu River;

³ JZ water were sampled from Jinze Reservoir; *FCs were presented in the unit of colony forming unit (CFU)/mL-water.

†pH of Taipu River samples kept at 6.95 – 7.03 during the whole period of study.

#Parameters having a *P* value lower than 0.1 in the rda forward section to explain the variations of resistome were listed, and the AIC index were provided along the with significant variables

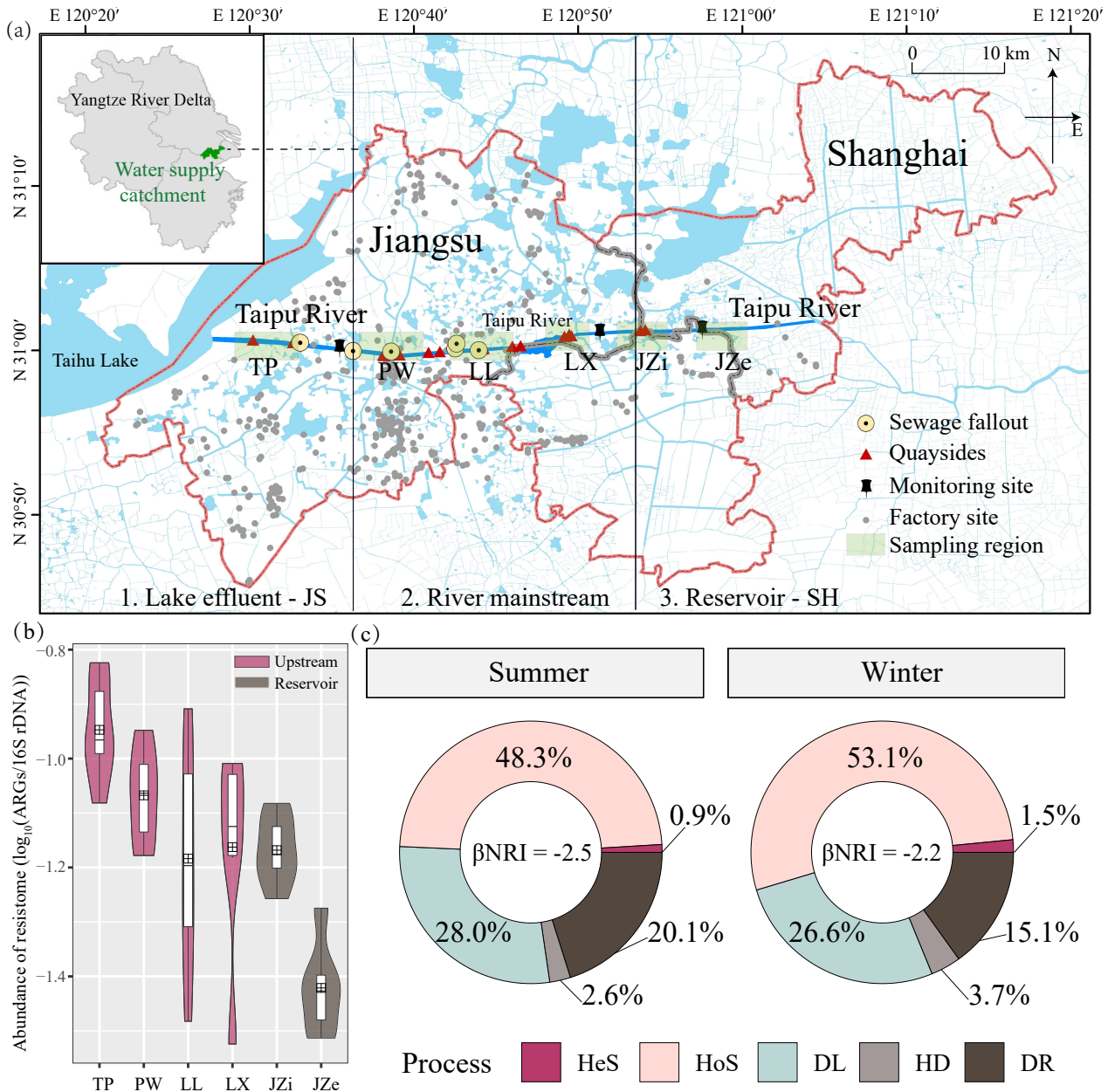


Fig. 1 (a) Taipu River functions as a canal that connected Taihu Lake in Jiangsu Province and Jinze Reservoir in Shanghai. The flow rates of the catchment were managed by the pumping stations on the Taipu River. (b) Samples were collected from six regions along the catchment (in green shades) including Taihu Lake pumping stations (TP), Pingwang Station (PW), Lili Station (LL), Luxu Station (LX), Jinze Reservoir influent (JRi), and Jinze Reservoir effluent (JRe). The relative abundance of resistome in each site was averaged during the whole period of study, and the boxplots denoted in the same color were statistically the same. (c) the iCAMP-estimated relative importance of different microbial ecological assembly processes and the homogeneous selection (HoS) had predominant influences over heterogeneous selection (HeS), dispersal limitation (DL), homogenizing dispersal (HD) and drifting (DR), which suggested strong environmental filtering effects on the deterministic bacterial assembly process ($|\beta\text{NRI}| > 2.0$).

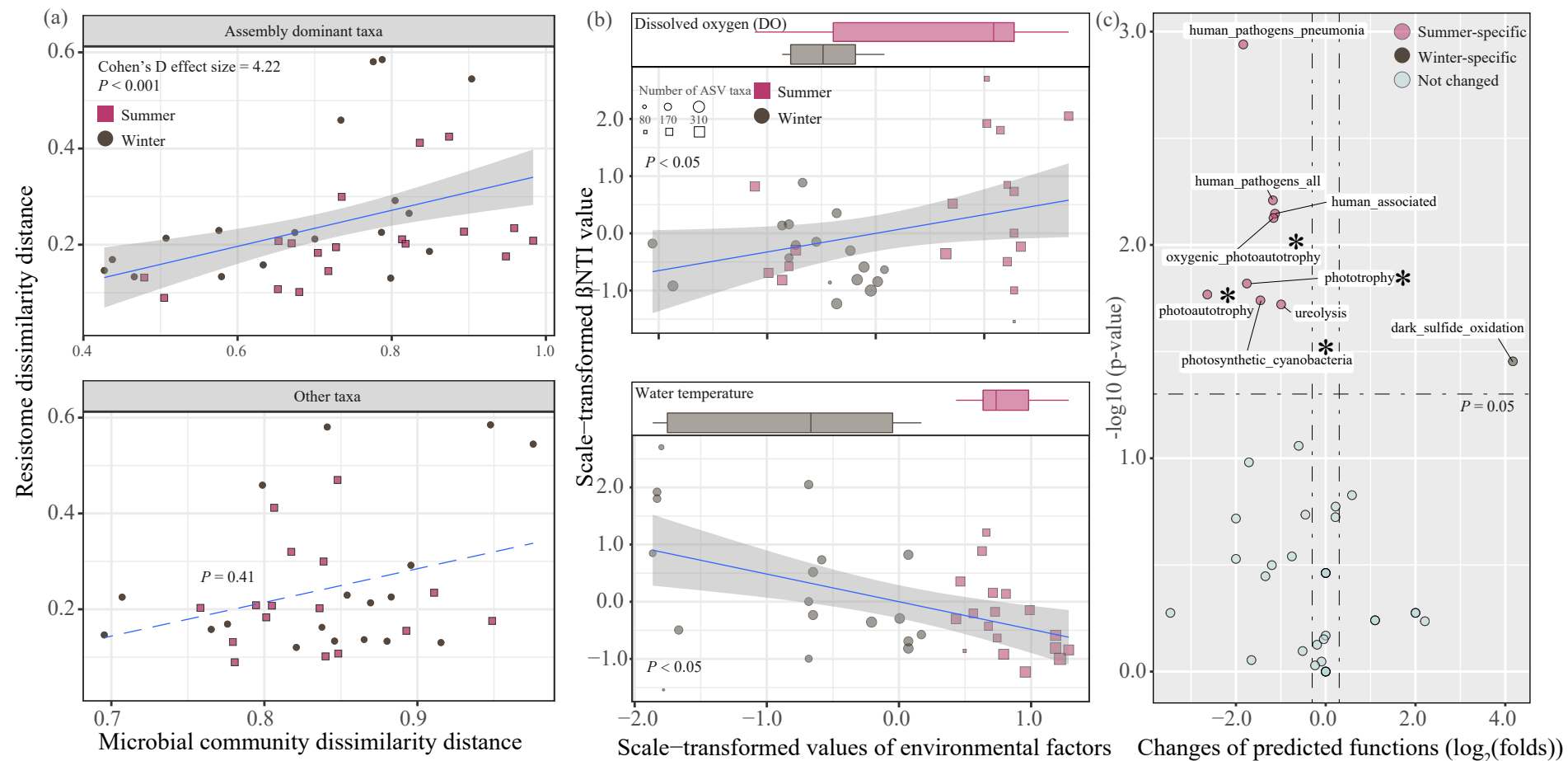


Fig. 2 (a) Correlations between bacterial community structures (assembly - dominant taxa vs. others) and compositions of antibiotic resistomes in each sampling site along the catchment (Bray-Curtis transformed distance). (b) Linear regression between the identified environmental factors (DO and temperature) and beta nearest-taxon-index (β NTI). (c) Microbial metabolic functions predicted by FAPROTAX. Pathways had significantly higher intensity in summer and winter were depicted in red and grey (Wilcoxon rank-sum test, $P < 0.05$), respectively. The pathways detected as seasonal variation representative ones using lfse analyses (LDA = 3.0) were annotated with an asterisk.

Figure 3

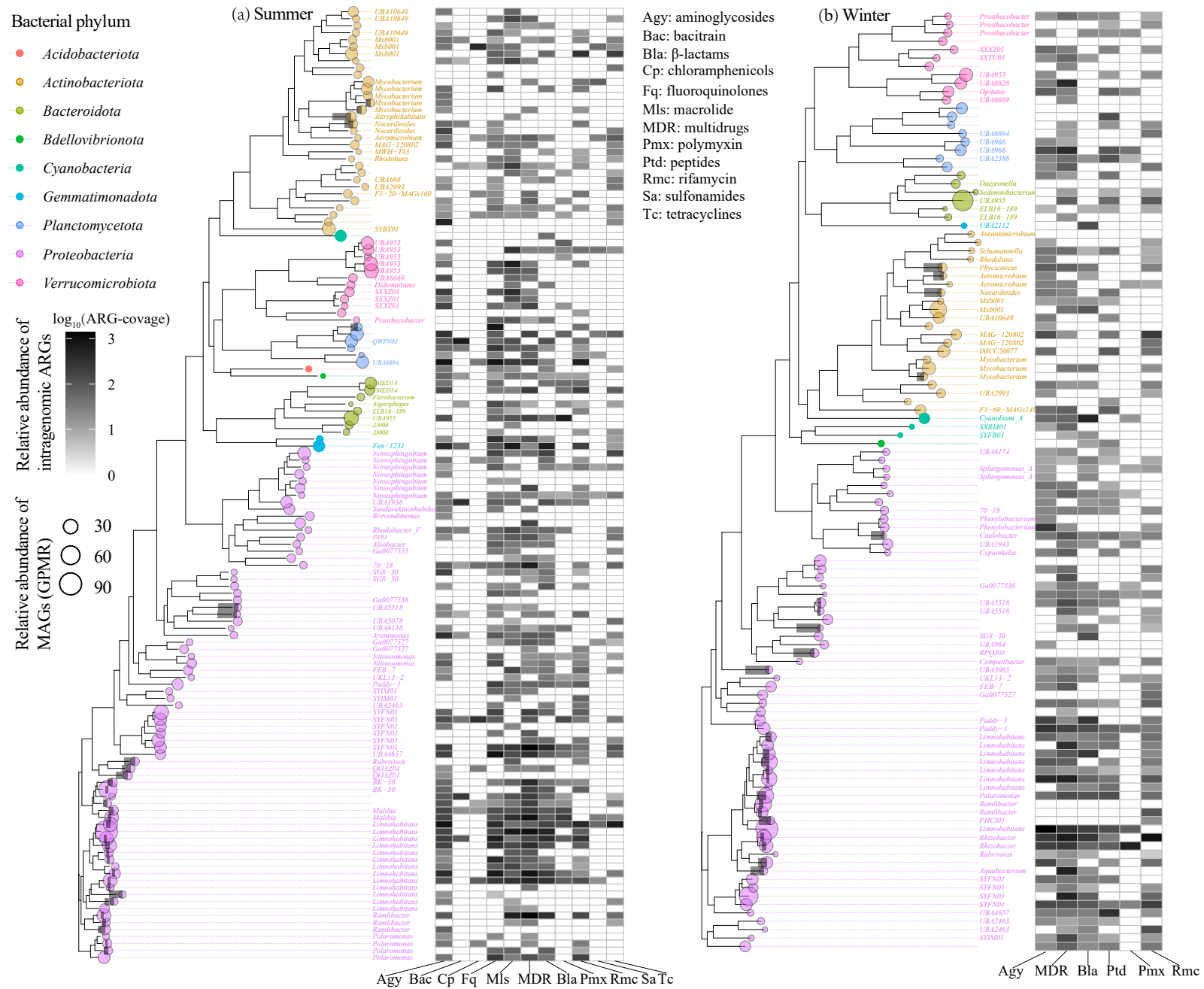


Fig. 3 Distribution and phylogenetic trees of the assembled ARGs-hosting metagenome-assembled genomes (MAGs) in summer **(a)** and winter **(b)**. The MAGs of taxa belonging to the same phylum were denoted in the same color. Among them, genomes that were identified as putative resistant pathogens were depicted in grey shades. The relative abundances of the MAGs (GPMR) are shown in proportion to the size of the nodes in the phylogenetic trees. The relative abundance of intra-genomic ARGs was shown in heatmaps.

Figure4

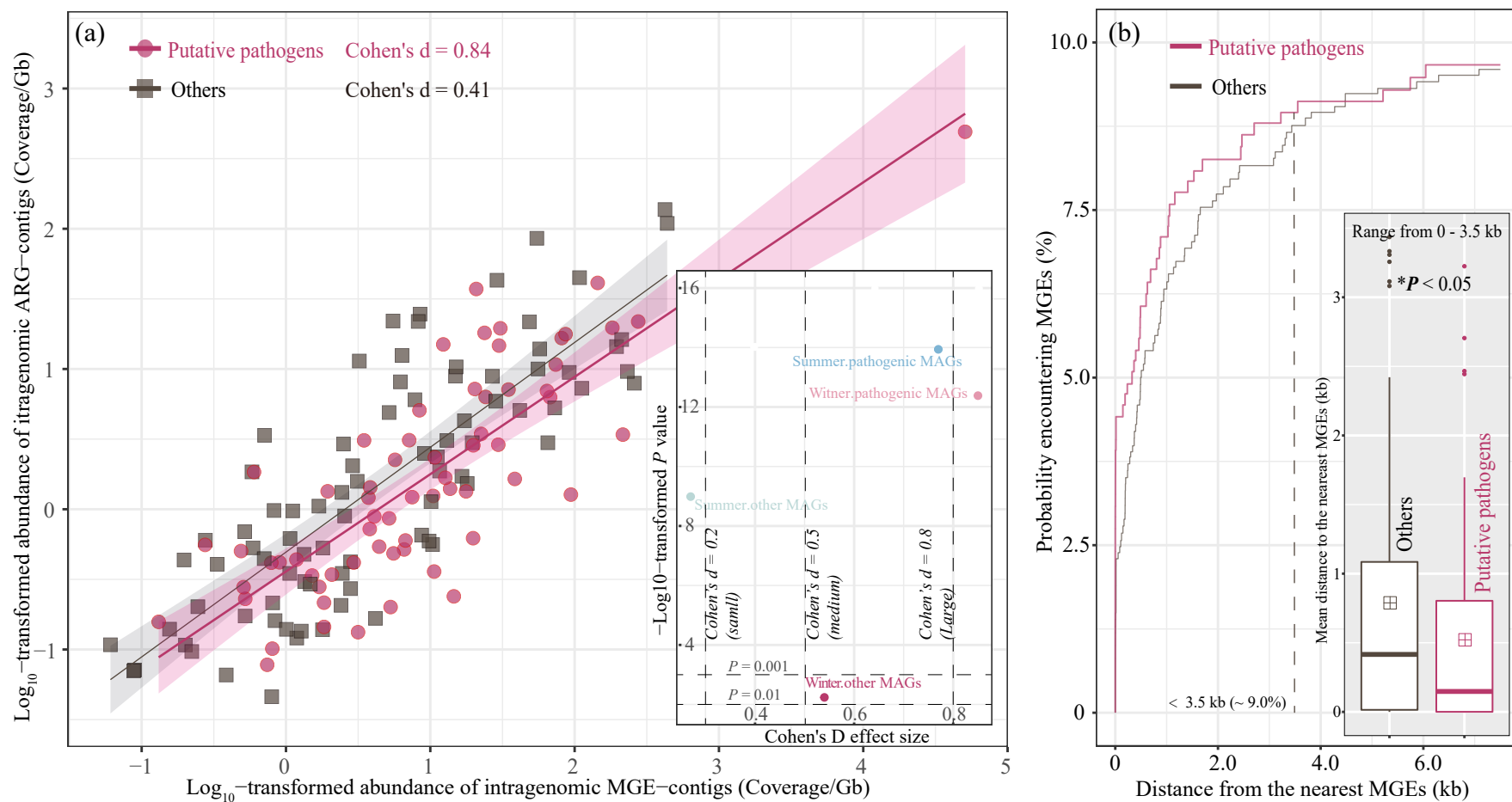
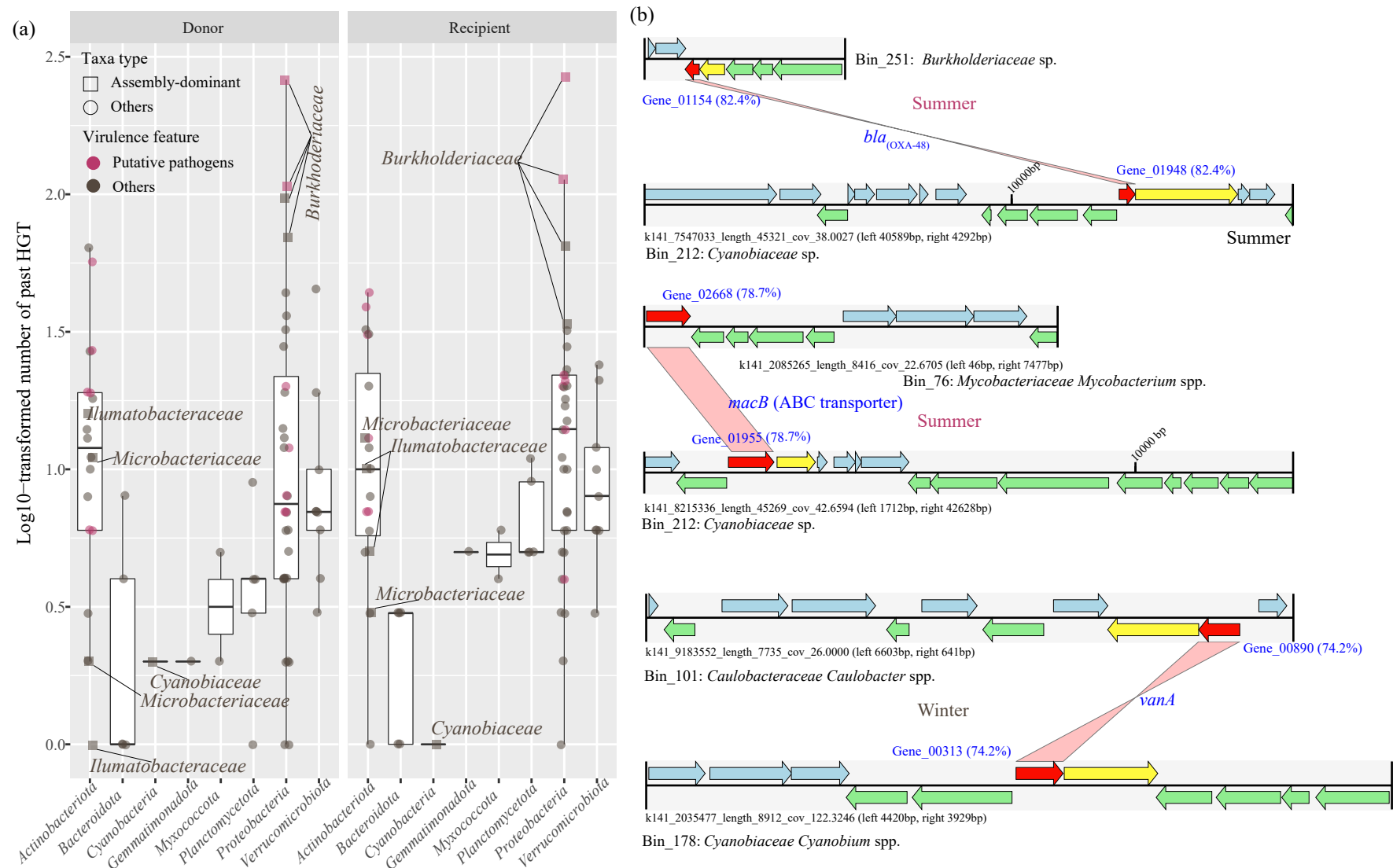


Fig. 4 Linear regression between the abundance of intragenomic MGEs and ARGs in summer and winter samples **(a)**; the Cohen's D effect sizes representing the closeness of regressions between subgroups intragenomic ARGs and MGEs were plotted in the subpanel. **(b)** The metagenome-assembled genomes (MAGs) representing human virulent putative pathogens and others were denoted in red and grey, respectively. The probability of the horizontal gene transfer (HGT) of ARGs across the MAG-assemblages was represented by the incidence of encountering the nearest MGEs. The MAGs of putative pathogens exhibited significantly greater potential HGT of ARGs relative to other genomes within the nearest (ARG - MGE) matching-pair distance of 3.5 kb.



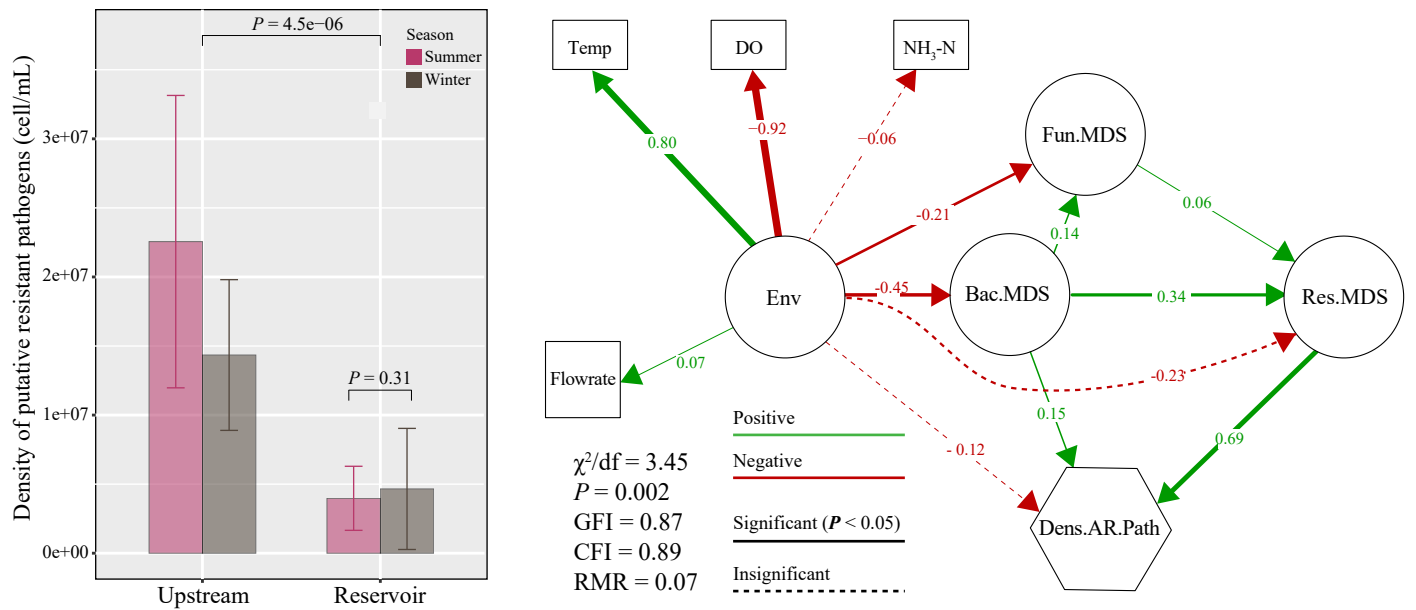


Fig. 6 (a) Mean of cell densities of putative resistant pathogens in the upstream and drinking water reservoir samples collected from the Taipu River Catchment. **(b)** Structural equation modeling (SEM) analysis of the impacts of forward-selected environmental factors (Env), structure (Bray-Curtis multidimensional scaling components) of microbial assembly - dominant taxa (Bac.MDS) and antibiotic resistome (Res.MDS) on the variations of cell densities of waterborne putative resistant pathogens (Dens.AR.Path) in catchment. In the constructed SEM, the co-variances among Env, predicted microbial metabolic functions (Fun.MDS), Bca.MDS and Res.MDS were considered. The relationships fitting a significant correlation ($P < 0.05$) either in positive (green) or negative (red) is depicted using a solid line. The width of lines are in proportion to the standard path coefficients (std-coeff β).



Click here to access/download

**Electronic Supplementary Material (for online publication
only)**

SI_WaterSupplyCatchement.docx